Advances in Science and Technology Research Journal

Advances in Science and Technology Research Journal 2023, 17(4), 21–35
https://doi.org/10.12913/22998624/167456
ISSN 2299-8624, License CC-BY 4.0

Received: 2023.05.05
Accepted: 2023.06.06
Published: 2023.08.12

Application of Laboratory Tests in Numerical Analysis for Exhaust Emissions in Business Jet Engines

Adam Kozakiewicz[1*], Aleksandra Kołodziejska[1], Rafał Kieszek[1]

[1] Institute of Aircraft Engineering, Faculty of Mechatronics, Armament and Aviation, Military University of Technology, ul. S. Kaliskiego 2, 00-908 Warszawa, Poland

* Corresponding author's e-mail: adam.kozakiewicz@wat.edu.pl

ABSTRACT

This article deals with the exhaust emissions from aircraft turbine engines, which is related to the rapidly growing market for this type of aircraft and its contribution to toxic emissions. The test carried out was done on a business jet turbine engine exhaust pollutants. The test object was the DGEN 380 engine. In order to determine the toxic composition of the exhaust gas as a function of the engine's operating range, an experiment related to the actual engine was conducted in the first stage. The test performed on the static thrust stand of the DGEN 380 turbine engine provided the necessary data on the parameters of the working medium for further research. The actual rotational characteristics of the engine were obtained. It was also determined numerically using GasTurb software. A high correspondence between experimental and calculated parameters was obtained, which gave the possibility of using them in further analyses of the exhaust gas pollutants of the studied engine. The correspondence of the results showed the correctness of the computational model built, thus predestining it for use in further analysis. This paper presents a model of the reverse-flow combustor made for numerical thermal-fluid studies. The thermal-fluid analysis of the model was performed in the ANSYS Fluent environment. The calculations were performed for three shaft speed. The numerical analysis provided information on changes in pollutant components of the exhaust gas of the DGEN 380 aircraft turbine engine as a function of changes in the shaft speed range. The results showed that the levels of nitrogen oxides depend greatly on shaft speed. The model built and the numerical analyses conducted also provided information about the zones inside of liner casing that affect significantly the amount of pollutant compounds obtained, which can then be used in the work on improving the design in terms of reducing the engine exhaust pollutants.

Keywords: aviation turbine engine, the reverse-flow combustor, engine exhaust pollutants, NOx reduction, turbine engine performance map.

INTRODUCTION

According to a study by the European Environment Agency, air transport accounts for nearly 3.5% of greenhouse gas emissions in the European Union. This is a significant figure, and it is important to note the fact that emissions have been steadily increasing, amounting to almost a 130% increase over the past two decades [1]. This allows us to conclude the demand for research in this area, with the aim of reducing further increases in pollutants emissions from aircraft turbine engines.

The largest concentrations of exhaust fumes are areas near airports, but also the stratosphere and the ozone layer. Standards for pollutants emissions from jet engines are already in place; however, they only apply to units with a thrust above 27 kN [2]. Low thrust jet engines and reciprocating engines are still not covered by the standards. The rise in popularity of the so-called "air cabs", and private single-engine jets, further increases the negative impact of aviation, now and in the future, on the environment. Excessive carbon dioxide emissions are known to increase the greenhouse effect, while nitrogen

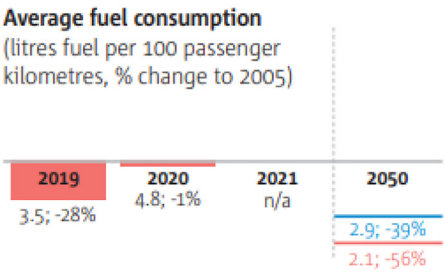

Fig. 1. Predicted fuel consumption over the next few years [4]

oxides contribute to the reduction of the ozone layer, smog formation and respiratory diseases. Harmful components also include unburned hydrocarbons and particulate matter, which are also responsible for the formation of smog, and have carcinogenic effects [3]. World and European organizations continue to work on analyzing these phenomena. In 2022, EASA released a report forecasting emissions until 2050. Fuel consumption is expected to decrease between 39–56%

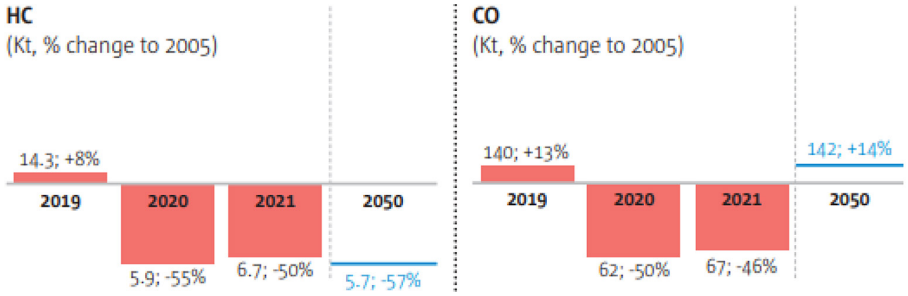

Fig. 2. Predicted CO and UHC emissions over the next few years [4]

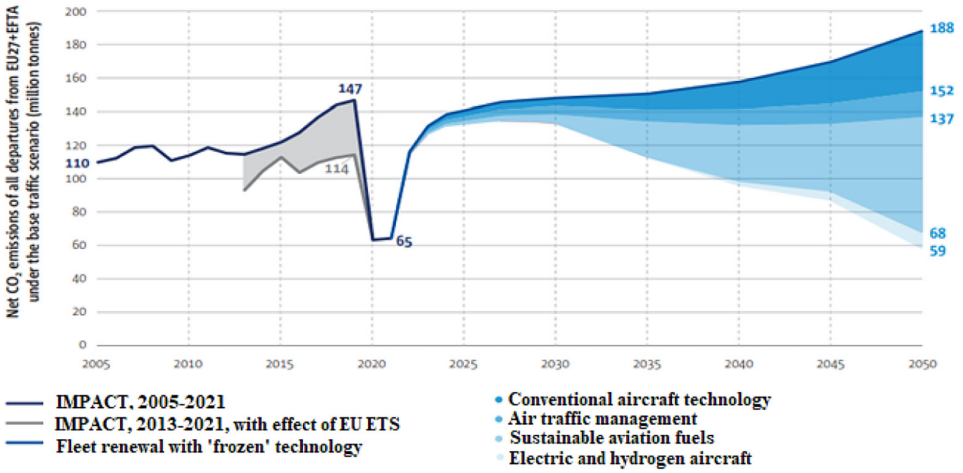

Fig. 3. Predicted CO2 emissions over the next few years [4]

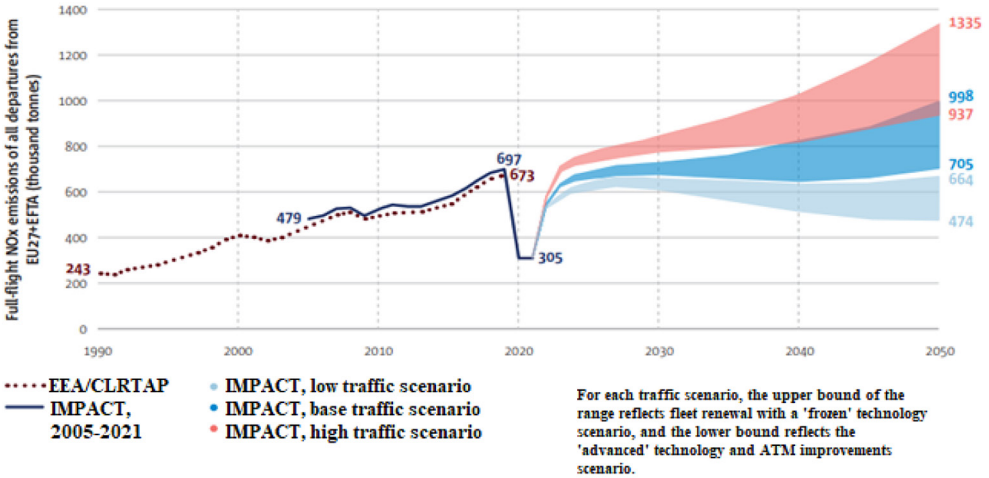

Fig. 4. Predicted NOx emissions over the next few years [4]

(compared to 2005), depending on the use of new technologies (Fig. 1). Unburned hydrocarbon emissions are also expected to decline slightly. However, carbon monoxide emissions are also expected to increase by about 14% (Fig. 2). In the case of carbon dioxide, the report predicts that there could be a 71% increase in emissions without the use of new technologies, and with the use of new technologies these emissions could be reduced by as much as 47% (Fig. 3). With nitrogen oxides, they are expected to increase from 47% up to as much as 108% (Fig. 4) in the absence of the use of new technologies [4].

The problem concerning the reduction of pollutants and the amount of exhaust gas is being solved in three main [18, 19]:

- converting jet fuel to one that produces lower levels of pollutants compounds [21, 22, 25],
- modification of aircraft takeoff and landing profile, [20, 23, 24], to protect the airport perimeter area,
- modernizing the design, such as by introducing variable geometry [18, 26],
- changes in the organization of the combustion process on the basis of studies of the operation of combustion chambers [27].

TESTS OF ENGINE OPERATING PARAMETERS

In view of the rapidly growing market for this type of aircraft and its contribution to pollutant exhaust emissions, an attempt was made to study a turbine engine of a business jet in terms of the pollutants of its exhaust, in the fourth area concerning the possibility of changing the organization of the combustion process in the combustion chamber. The test object was the DGEN 380 engine (Fig. 5), manufactured by the French company Price Induction. DGEN is an engine manufactured for light aircraft, so-called Personal Light Jets. It is a two-duct turbojet engine, characterized by its small size and weight. The engine was designed to reduce noise emissions, as well as reduce fuel consumption, which has a direct impact on reducing carbon dioxide emissions. JET A-1 fuel is used to power this engine [5]. The basic data of the engine is shown in Table 1.

In order to determine the toxic composition of the exhaust gas as a function of the engine's operating range, an experiment related to the actual DGEN 380 engine (Fig. 6) was conducted in the first stage. Such an engine is owned by the laboratory of the Faculty of Mechatronics, Armament and Aviation, Institute of Aircraft Engineering of the Military University of Technology and its tests were performed on a stationary static thrust stand located at the Air Force Institute of Technology in Warsaw. The engine is equipped with the FADEC system and ancillaries from Price Induction.

Table 1. DGEN 380 engine characteristics [5]

Parameter	Value
Thrust for Ma = 0.0	2.55 kN
Specific fuel consumption	0.44 lb/(h×lbf)
Thrust on the cruising range (Ma = 0.338)	1.05 kN
Bypass ratio of mass flow rate	7.6
Mass	85 kg
Maintenance interval	3 600 h

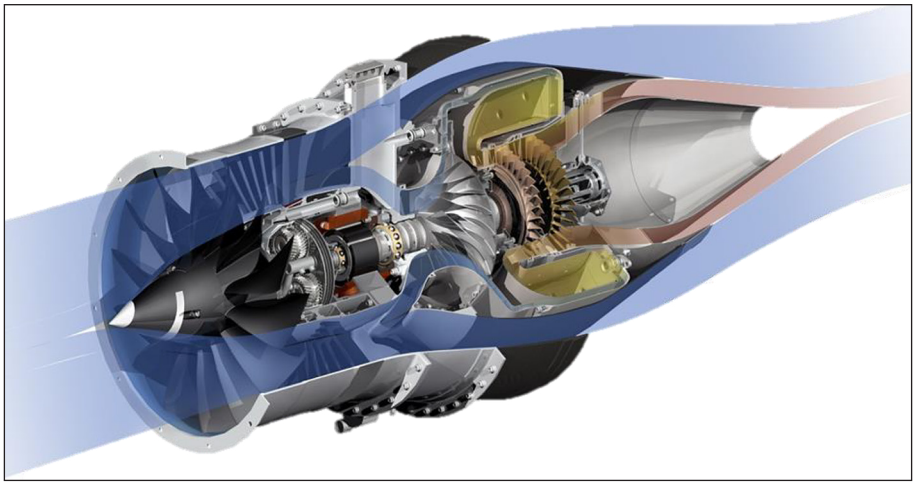

Fig. 5. Design of the DGEN 380 engine [5]

Fig. 6. DGEN 380 engine integrated on a static thrust stand

A typical engine test program was performed, which included:

- startup (idle range),
- takeoff range,
- checking the specific engine operating parameters,
- acceleration control,
- engine cooling and shutdown.

The engine has been placed on a stably fixed frame and a pylon, which are aligned with the axis of the tunnel (Fig. 6). The engine is located on the pylon by means of a mechanical connection. The pylon itself is equipped with a sensor responsible for measuring thrust values, as well as oil and fuel installations. The fuel system is connected to a room called the control room. A schematic of the test stand is shown in the Fig. 7.

Pressure measurements are taken inside the engine through either 1.6 mm diameter capillaries or 4 mm diameter polyamide tubes. Each pressure measurement is associated with a pressure sensor, located in a cabinet containing all the engine sensors. Thermocouples are used for temperature measurements. Some of them are permanently installed in the engine, while others can be additionally connected. In addition, flow parameters are used for measurements, and rotor and pump speeds are read by FADEC, the electronic motor control system.

Price Iduction's equipment is connected to the electrical grid located in the building via an electrical box. It transfers all the measurement data from the sensors to it and ensures that it is sent to the control panel. The data is presented on screens. The control room is also where the process of controlling the motor thrust takes place, using the PLA (Power Level Angle) lever.

WESTT CS/BV is a state-of-the-art workstation that simulates the operation and control

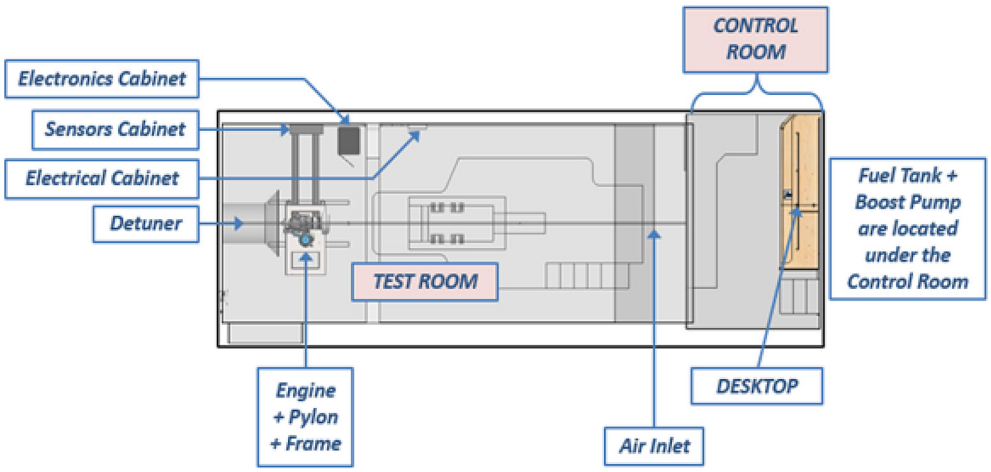

Fig. 7. Diagram of the DGEN 380 static thrust stand

system of the DGEN 380 engine. The workstation is built with:

- two PCs and three monitors (2 for PC1 and 1 for PC2);
- an engine simulation system;
- an engine control system (FADEC - Full Authority Digital Electronic Control);
- a system that connects the work of FADEC and PC1;
- motor control panel;
- communication panel.

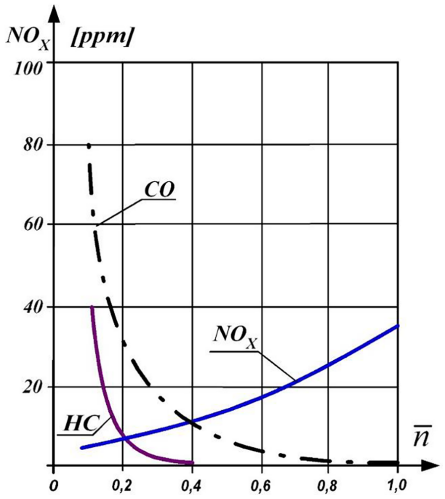

Fig. 8. Effect of relative rotor speed on pollutants composition of exhaust gas, where $\bar{n}$ = relative rotor speed [8]

The static thrust stand test performed on the DGEN 380 turbine engine was to provide the necessary data (on the parameters of the working medium) for further research. The engine's operating range affects the amount of pollutant exhaust components (of each type) emitted for all types of turbine engines [9, 10, 13]. An increase in engine spool speed is accompanied by an increase in the amount of NOx released with a decreasing amount of CO and unburned HC hydrocarbons (Fig. 8). This process occurs with both turbine jet engines and turbine propeller and helicopter engines. The selection of the speed range is important for the airport area [12], since the operating range of turbine engines in this area is associated with operation at high rotor speed values (on average above 60%).

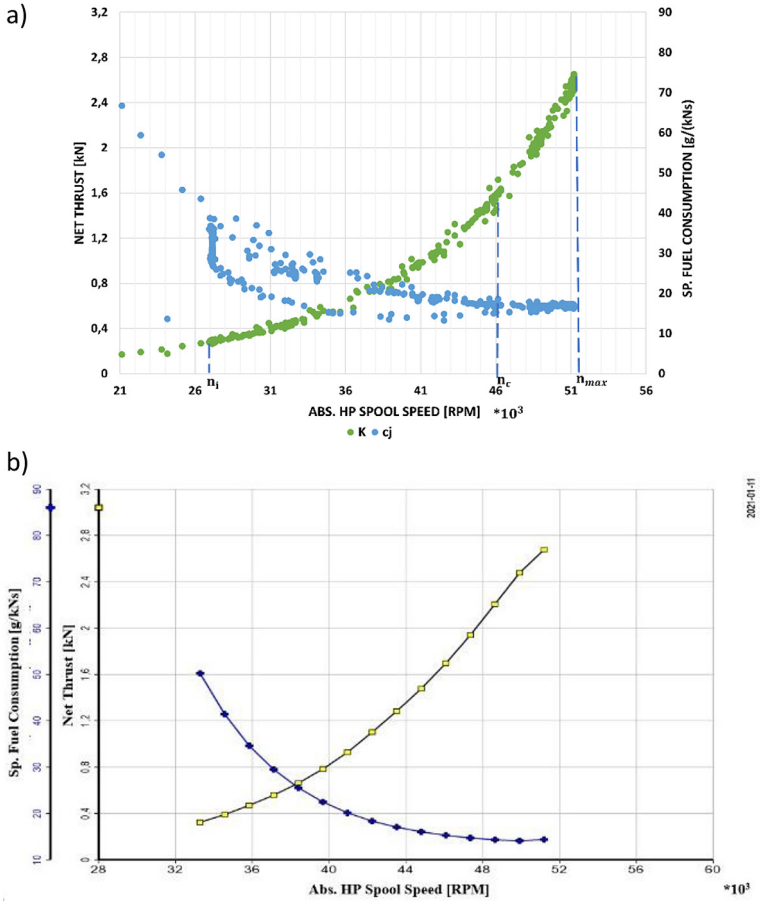

Fig. 9. Dependence of thrust and specific fuel consumption on the speed of the high-pressure rotor for a) testbench b) GasTurb analysis, where: n_j - idle speed, n_c – cruise speed, n_{max} – maximum speed

The engine test carried out provided a range of data in terms of the thermogasodynamic parameters of the engine's working medium, and the actual rotational characteristics of the DGEN 380 engine were obtained, i.e. the changes in thrust and specific fuel consumption as a function of shaft speed (Fig. 9a). It was also determined numerically using GasTurb software. The data obtained numerically (Fig. 9b) largely cover the experimental (true) data. It can be seen that there was a slight shift in the curves on the cruise range and design speeds, towards higher parameter values. The engine thrust obtained in the computer simulation is about 1.5% greater than the thrust obtained in real conditions, while the specific fuel consumption for maximum speed is much higher for real conditions, as the difference is about 15%.

In the case of numerical analyses, the results are presented from values above 32,000 rpm due to the fact that below this value the engine operates in transients, which is evident in the scatter of recorded parameters during the experiment (e.g., Fig. 10 a).

GasTurb software was also used in order to determine the necessary parameters for the numerical testing of exhaust gas pollutants. The obtained results, i.e. the numerical map, were checked and compared with the experimental results (Fig. 10 and Fig. 11).

The first parameter, and the primary one, which was subject to checking is the temperature before the turbine , which affects the pollutants of the exhaust gas because it is a consequence of the combustion temperature. Under real conditions (Fig. 10a), as well as during simulation in the software (Fig. 10b), the exhaust gas temperature at the turbine inlet reaches its maximum near 1400 K for maximum shaft speed values. At the same time, the minimum temperatures shown in the graphs oscillate around 1000 K. In the cases of the model simulated in the GasTurb environment, its range is shifted to a slightly higher shaft speed range. The maximum temperature at the exit of the combustion chamber, which occurs on the range of maximum shaft speeds, in real conditions is about 1.5% higher than the simulation in GasTurb.

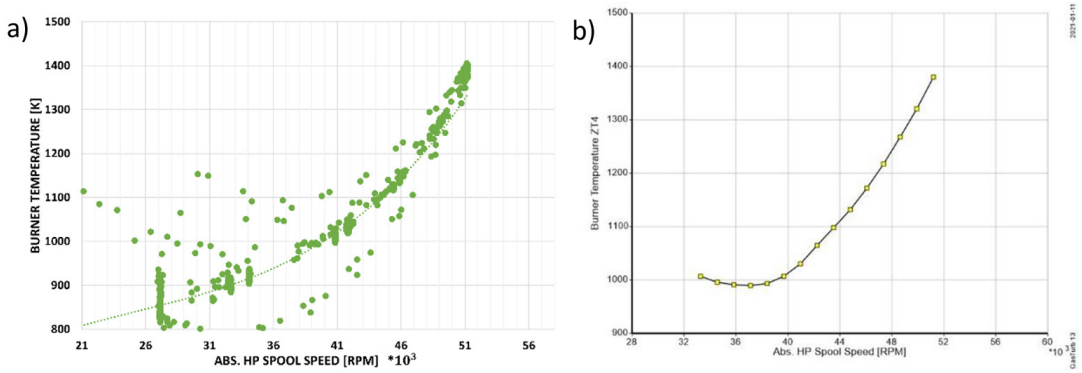

Fig. 10. Dependence of exhaust gas temperature at the turbine inlet on the speed of the high-pressure rotor, where: a) data measured in the engine, b) calculated results from the GasTurb program

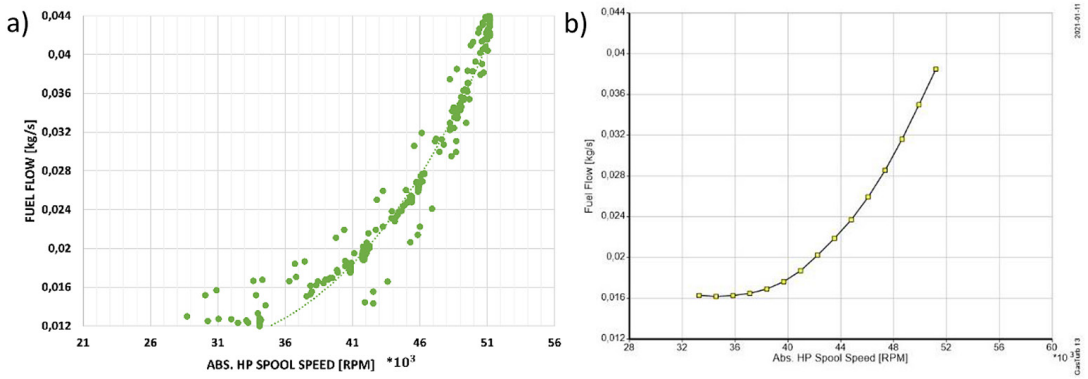

Fig. 11. Dependence of second fuel consumption on the speed of the high-pressure rotor, where: a) data measured in the engine, b) calculated results from the GasTurb program

Another parameter important in terms of the criterion of exhaust gas pollutants is the value of fuel consumption [11] per unit time. The obtained characteristics for the dependence of second fuel consumption on spool speed also show considerable similarity in both cases, test cell value (Fig. 11a) and calculated (Fig. 11b). The minimum second fuel consumption is about 0.01 kg/s for this engine and occurs at a speed of about 32,000 rpm (idle speed). On the engine's maximum speed range (51,000 rpm), it reaches values of about 0.04 kg/s. Actual fuel consumption is 11% higher than that determined by GasTurb software.

A high correspondence between experimental and calculated parameters was obtained, which gave the possibility of using them in further analyses of the exhaust gas pollutants of the studied engine. Both the combustion chamber exit temperature, fuel consumption, as well as thrust and specific fuel consumption show a similar pattern of actual (obtained on a static thrust stand) and numerically determined rotational characteristics. This indicates the correctness of the computational model built, thus predestining it for further analysis of the effects of engine operating parameters on CO, CO_2 and NOx emissions.

MODEL DESIGN

The authors have access to two DGEN 380 engines, the first of which is mounted on the test stand and was used for experimental research. The second was dismantled and, based on its geometry and technical documentation, a model of the reverse-flow combustion chamber was made (Fig. 12). DGEN 380 engine was fueled with JET A-1. The three-dimensional model of the chamber was made using Siemens NX software. A numerical simulation based on the Finite Volume Method was performed to determine the changes in individual parameters in the chamber during combustion and to determine the emissions of specific exhaust components. The combustion process is very complex and poses many computational problems that necessitate replacing quantitative analyses with qualitative analyses at this stage of the research.

The structural system of the combustion chamber of the DGEN 380 engine consists of a liner casing having small-diameter cooling holes on the surface. The air casing and the liner casing is a strength system for carrying various types of loads. 13 air inlets were modeled at the entrance to the combustion chamber, along with dual flow swirlers. The chamber is also equipped with 24 zone holes for primary air and 24 holes for secondary air. The combustion chamber system is an axially symmetrical system; due to the distribution of elements of the component, the whole system can be divided into 13 periodic component sections; the software used makes it possible to account for interference between successive model elements. This provides the opportunity to perform numerical analysis for a repeated section of the combustion chamber in the form of a 2D model. The generated computational grid consists of 21,758 elements (Fig. 13). In order to increase the quality of the mesh, boundary layer compaction was applied near the model walls, which is fundamental in performing accurate numerical simulations. The thermal-fluid analysis of the model was performed in the ANSYS Fluent environment.

The calculations were performed for three engine shaft speeds:

- idle speed – 53.0%,
- cruise speed – 88.7%,
- maximum speed – 100.0%.

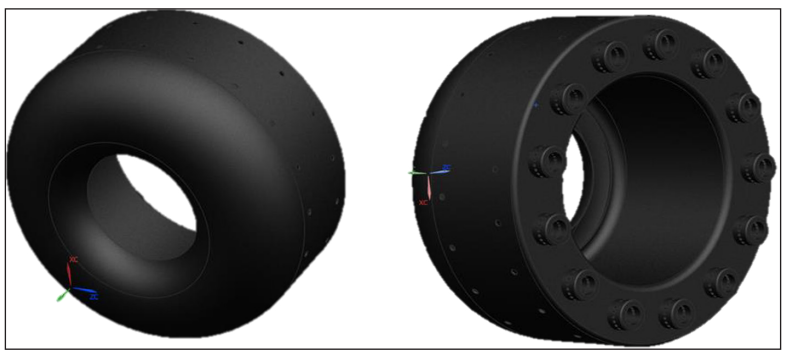

Fig. 12. Combustion chamber model

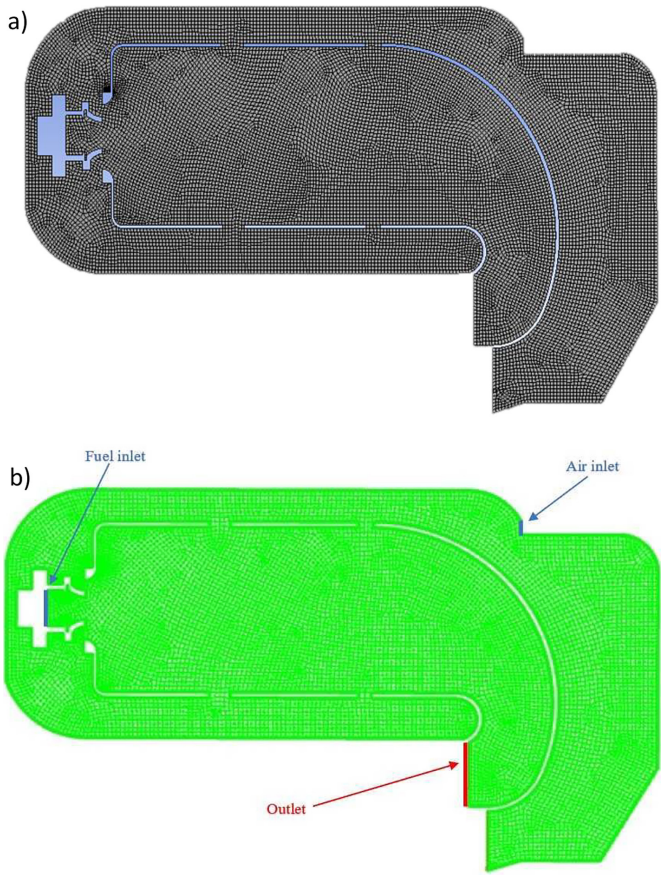

Fig. 13. Computational grid (a), and boundary conditions (b), based on Table 2

The engine operating parameters at these ranges were determined using the GasTurb program and are shown in charts Figure 14 and Figure 15. The defined boundary conditions for each of these rotational speeds and the basic settings of the numerical model are included in Tables 2 and 3.

Chemical equilibrium was also assumed and a probability density function was used with the ability to calculate 25 chemical components,

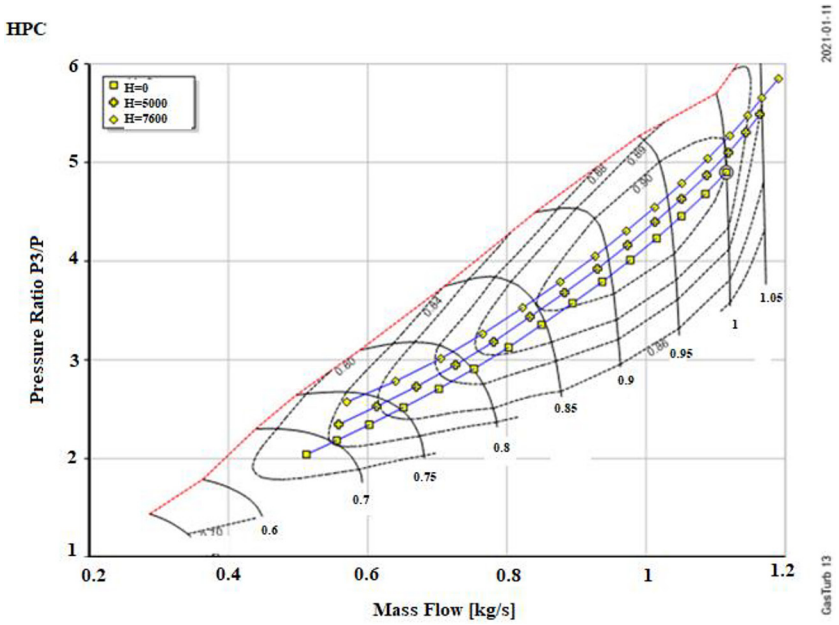

Fig. 14. Map of a high-pressure compressor

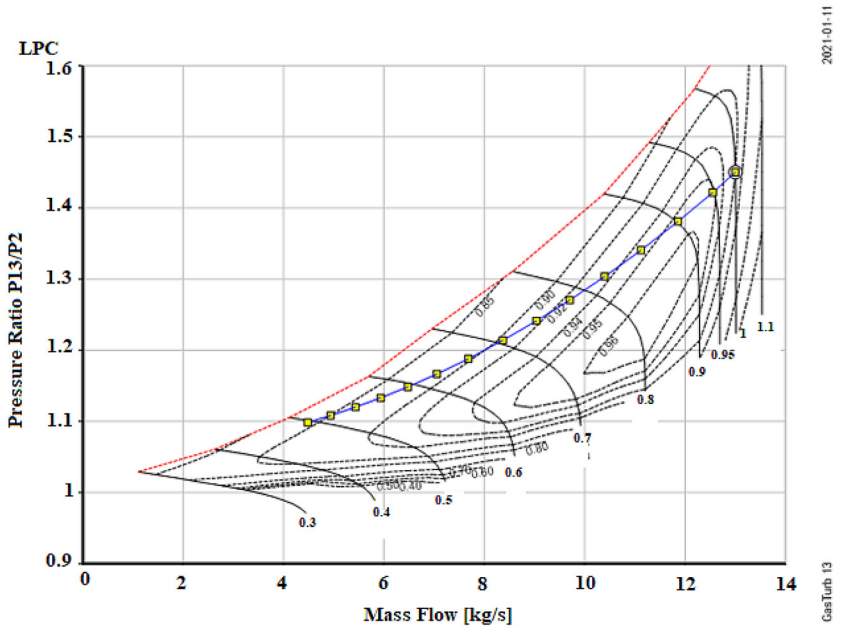

Fig. 15. Fan map (under static conditions H = 0)

Table 2. Boundary conditions for one injector

Parameter	Air output	Fuel output	Pressure at entrance to combustion chamber
Shaft speed	$n = n_j$ = 27,145 rpm		
Boundary conditions	0.05 kg/s	0.00066 kg/s	92.41 kPa
Temperature	355 K	290 K	832 K
Shaft speed	$n = n_c$ = 45,392 rpm		
Boundary conditions	0.1 kg/s	0.0019 kg/s	343.9 kPa
Temperature	460 K	290 K	1117 K
Shaft speed	$n = n_{max}$ = 51,196 rpm		
Boundary conditions	0.13 kg/s	0.0034 kg/s	461.3 kPa
Temperature	508 K	290 K	1398 K

Note: n_j - idle speed, n_c – cruise speed, n_{max} – maximum speed.

Table 3. Combustion model settings

Turbulence model	k-ε
Radiation model	Discrete ordinates
Combustion model	Non-premixed

but the main area of interest was the combustion products NOx and CO2. The model was tested in the initial "cold" phase, and in the final stage a module was also used to calculate nitrogen oxide emissions. Thermal and super-equilibrium nitrogen oxides are taken into account for nitrogen oxide emissions.

RESULTS

The numerical analysis provided information on changes in the pollutants components of the exhaust gas of the DGEN 380 aircraft turbine engine as a function of changes in the engine speed range. The first parameter analyzed is carbon monoxide CO (Fig. 16–18). The results illustrate that the zones of origin and highest concentration of carbon oxides are located in the fuel-rich area, and therefore in the primary zone of the combustion chamber, immediately after the swirler. The zone and amount of carbon monoxide formation rise with increasing shaft speed, which is due to the greater amount of fuel delivered as the engine's operating range increases. As the speed increases, there is a change in the distribution of zones for obtaining CO, from the area of the input zone (the initial liner casing) the zone expands to the output zone (Fig. 18). In terms of values in zones, the smallest were obtained on the idle range, which can be thought to be the result of low engine load.

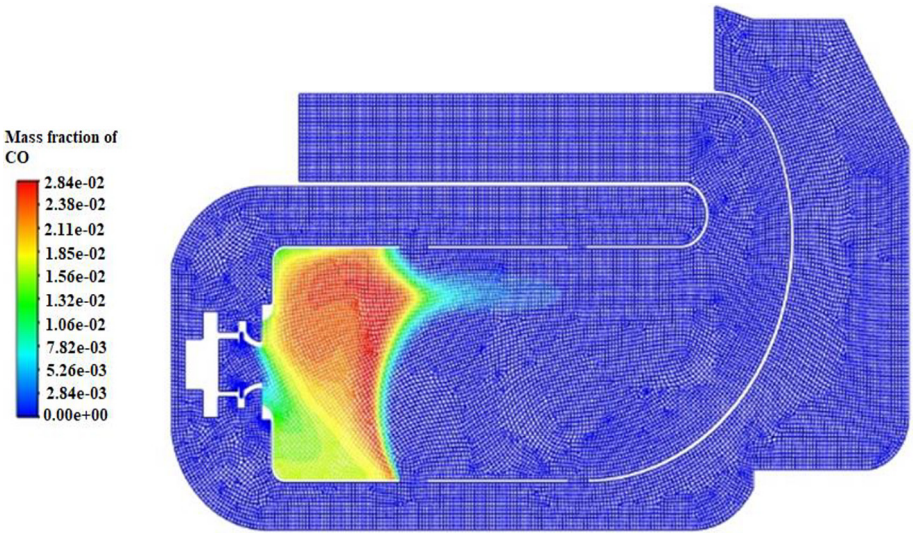

Fig. 16. Formation zones and CO emissions in the idle speed range

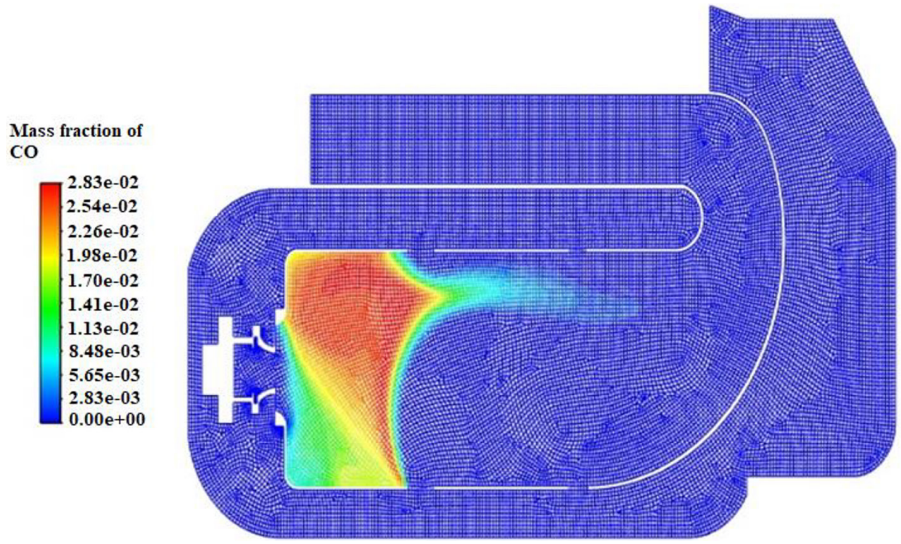

Fig. 17. Formation zones and CO emissions in the cruise speed range

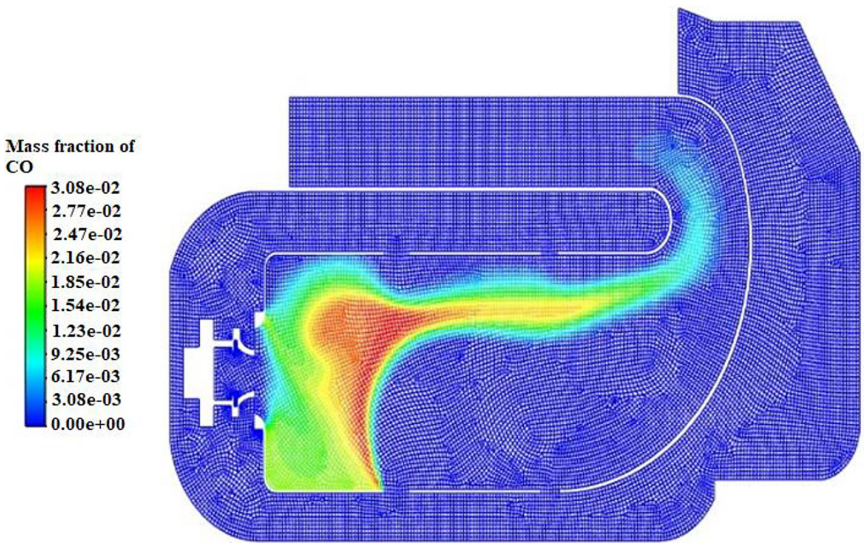

Fig. 18. Formation zones and CO emissions in the maximum speed range

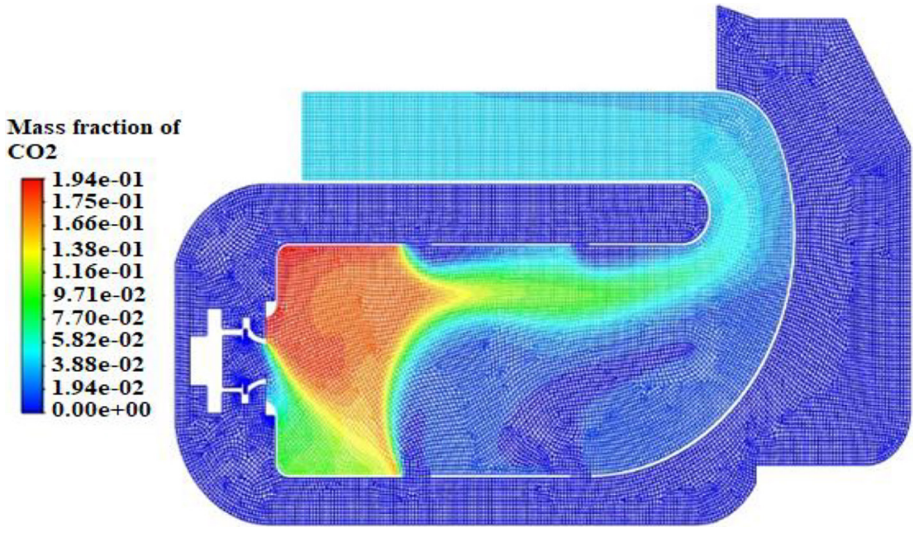

Fig. 19. Formation zones and CO2 emissions in the idle speed range

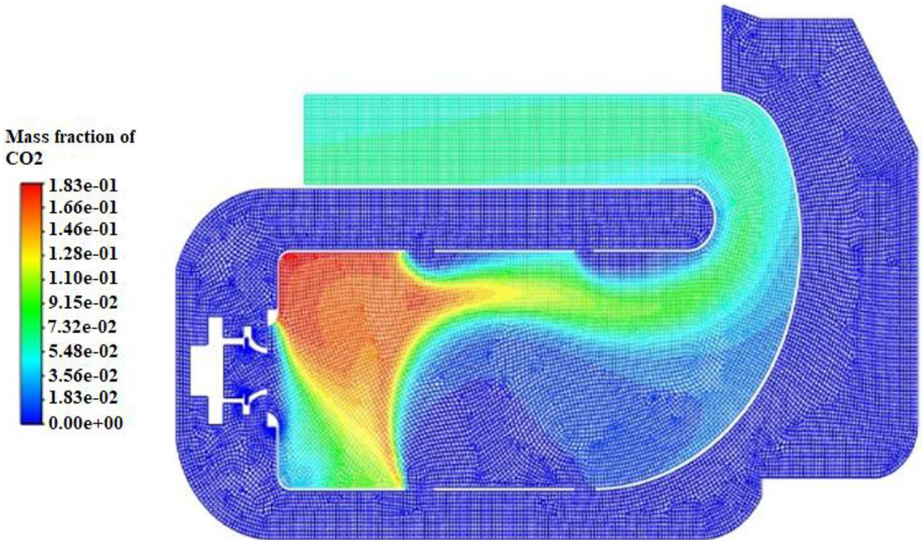

Fig. 20. Formation zones and CO2 emissions in the cruise speed range

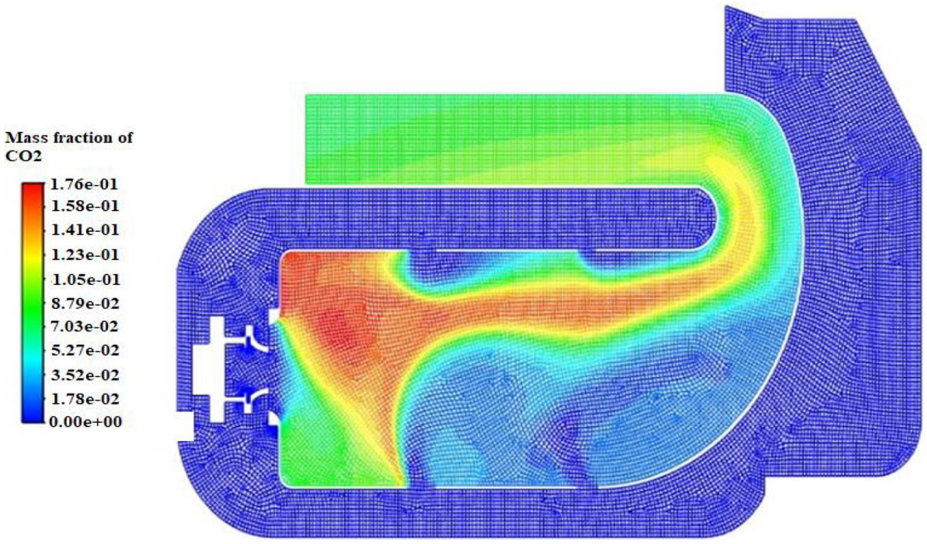

Fig. 21. Formation zones and CO2 emissions in the maximum speed range

The resulting percentage difference between the maximum range and the idle range is about 14%. On the other hand, there is only about 8% difference in CO between the maximum range and the cruising range.

The second parameter that was tested was CO2 (Fig. 19–21). The zone of the amount of carbon dioxide in the initial zone of the combustion fire tube decreases as the rotational speed increases, while the outlet zone is the largest for the range of maximum rotational speeds. The highest concentration of carbon dioxide observed in the initial zone of the combustion chamber may indicate the proper process of creating a combustible mixture by combining the fuel with the air stream and the correct combustion process. On the cruising range, the amount of carbon dioxide emitted into the atmosphere is nearly 40% less than when operating at maximum speed, while on the idling range the difference is 65%.

The most important parameter that gets the most attention during studies on exhaust gas pollutants is NOx. The amount of nitrogen oxides increases with shaft speed (Fig. 22–24), due to operation close to design conditions, and combustion close to complete. This is also due to the simultaneously increasing combustion temperature. It should be noted that thermal nitrogen oxides are formed at temperatures exceeding 1800 K. In the maximum shaft speeds range, the concentration of nitrogen oxides moves deeper into the combustion chamber (Fig. 24), resulting in

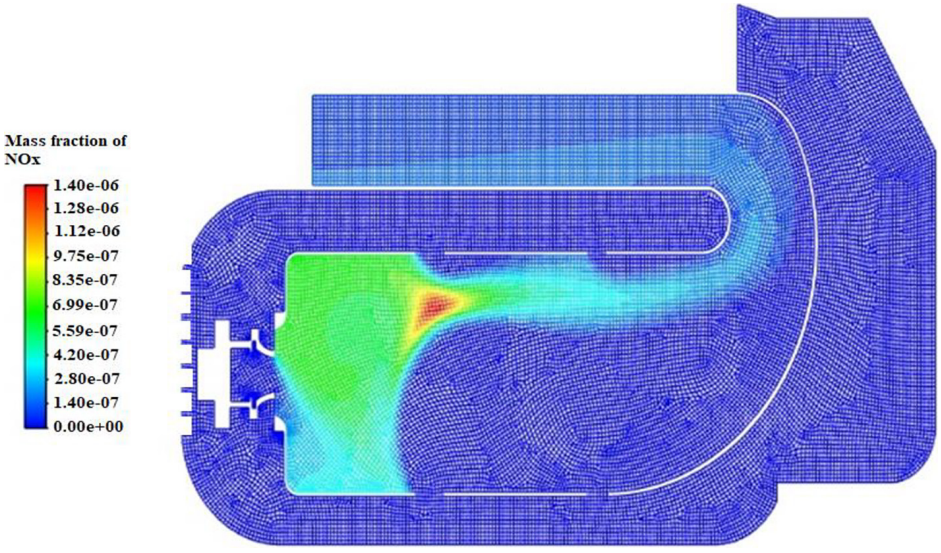

Fig. 22. Formation zones and NOx emissions in the idle speed range

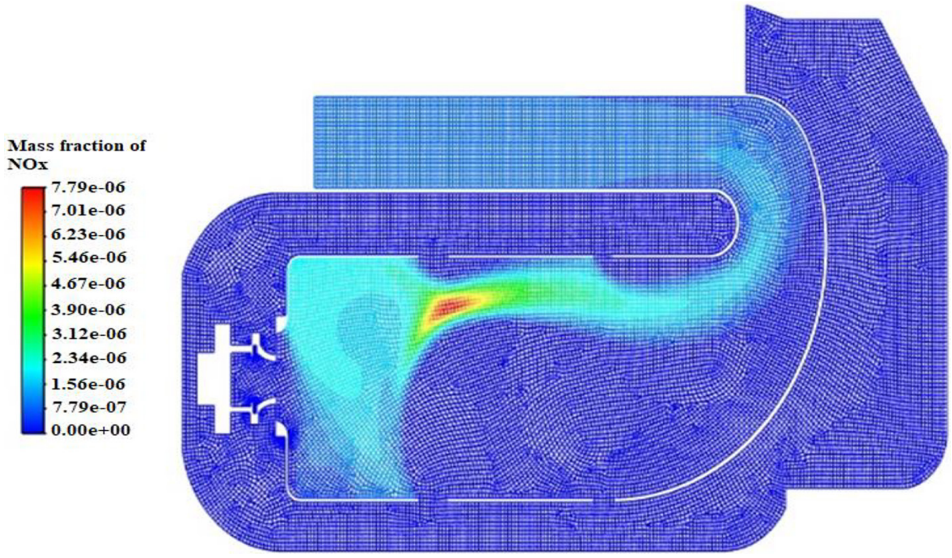

Fig. 23. Formation zones and NOx emissions in the cruising speed range

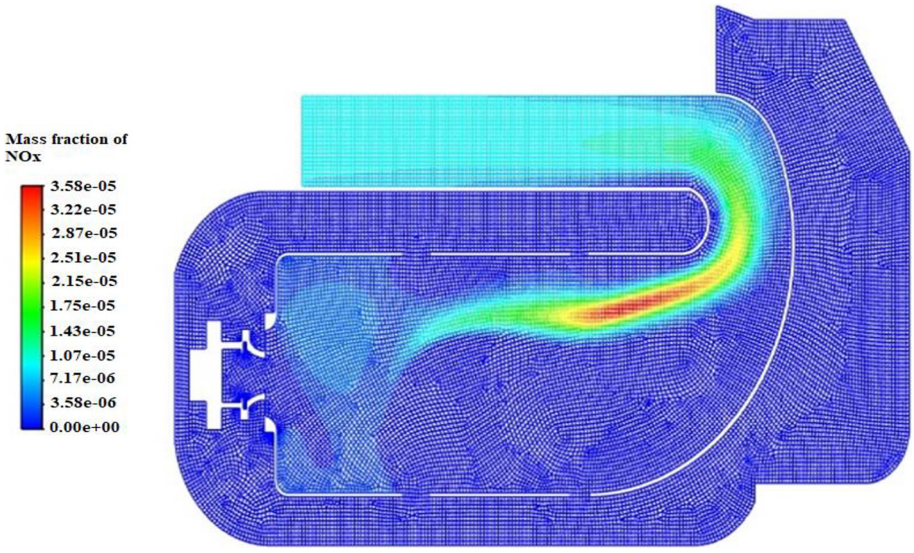

Fig. 24. Formation zones and NOx emissions in the maximum speed range

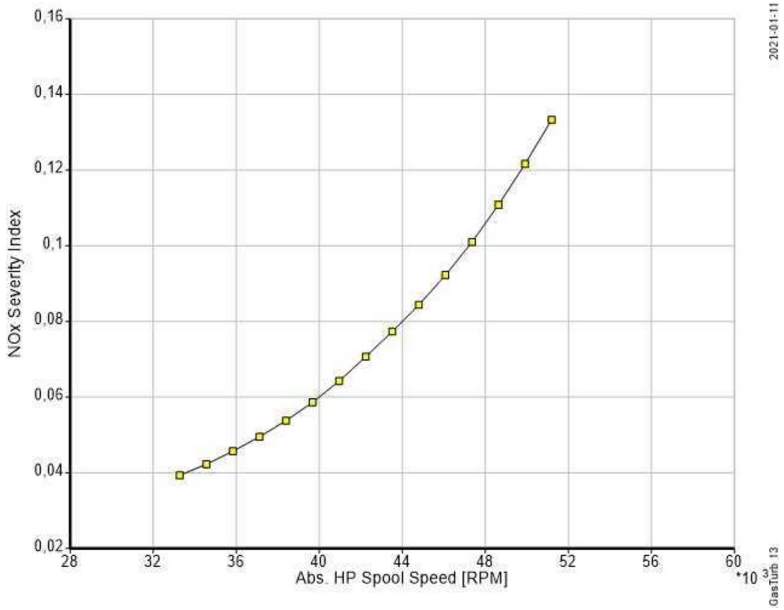

Fig. 25. Dependence of NOx emissions on shaft speed

increased emissions of these particles into the atmosphere. The change in the position of NOx formation zones shifts from the initial zone (Fig. 22) toward the end zone of the liner casing. The amount of nitrogen oxides on the maximum range (Fig. 24) compared to the idle range (Fig. 22) increases by as much as 99%, and compared to the cruising range (Fig. 23) is an increase of about 80%.

The combustion chamber results of the DGEN 380 engine are summarized in a characterization showing the effect of engine speed on NOx emissions (Fig. 25). The obtained graph shows that the amount of nitrogen oxides depends very strongly on the engine speed, which should force the use of a proper control algorithm or flight profile of the aircraft with the integrated DGEN 380 engine.

CONCLUSIONS

The present paper is part of a worldwide line of research concerning the ever-increasing greenhouse effect and the possibility of reducing it in the area of aircraft turbine engines. From the results presented in the paper, confirmation was obtained that for a new engine such as the DGEN 380, the greatest influence on pollutants exhaust

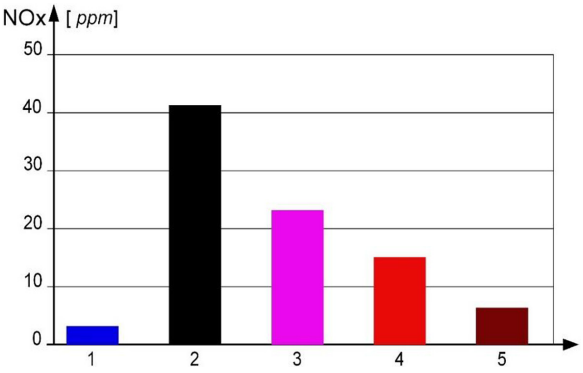

Fig. 26. NOx emissions depending on the methods used [8] (1 – catalytic combustion; 2 – water injection; 3 – steam injection; 4 – LPP (lean, premixed, prevaporized) combustion; 5 – LPP combustion selectively using catalysts)

emissions is exerted by the engine's operating range, i.e., speed, which translates into other engine operating parameters, among others, operating medium temperatures, excess air ratio in the combustion chamber and thrust. In addition, an important aspect is the quality of the fuel-air mixture, and therefore the process of fuel fragmentation and atomization [7]. Considering the operating time, the most pollutants can be generated during operation in the cruising range.

The numerical analyses performed and their high convergence (Fig. 9–11.) allowed us to conclude that the numerical calculations of pollution will also converge with the results obtained on the static thrust stand. This provides an opportunity for comparative analysis in terms of engine operation at different speed ranges. The results show a huge quantitative change in the NOx produced between the idle, cruise and maximum speed ranges. Moving the engine, between the two basic ranges, from the cruising speed range to the maximum range (a 12.8% increase) results in a 38.9% increase in the amount of NOx produced. Therefore, reducing the amount of these toxic compounds can be done through two routes. The first can involve reducing the maximum rotational speed. Changing the speed by even 1% can produce noticeable effects. The second possibility is that the model built and the numerical analyses conducted also provided information about the zones inside of the liner casing that affect significantly the amount of toxic compounds obtained, which can then be used in the work on improving the design in terms of reducing these products in case of the DGEN 380 engine. A variety of methods can be used for this purpose; for example, in order to reduce carbon monoxide and unburned hydrocarbons, it is advisable to fragmentate the fuel more finely and use pre-evaporation. In the case of nitrogen oxides, the stay time of the mixture in the combustion zone can be reduced, and efforts can be made to reduce the maximum flame temperature (e.g., water or steam injection – Fig. 26). Another way (design solution [3]) to improve the performance of the combustion chamber in terms of reducing NOx, CO and unburned HC hydrocarbons would be to redesign the chamber into a two-stage fire tube system (LPP-type combustion chamber). This allows the heat release rate ξ_{KS} to be kept high while idling. At maximum ranges, it gives large values of the excess air ratio α and a reduction in the amount of NOx produced. From the literature data, the use of a catalytic combustion system (theoretically) or a more practical system in the form of a combination of an LPP-type chamber with catalytic combustion can bring about a significant reduction in emissions of pollutants components of turbine engine combustion. Fully emission-free in the area of propulsion systems under study is only the electric system [14, 15, 16] or aircraft nuclear propulsion [17].

Acknowledgments

This research was funded by the Military University of Technology, Warsaw, Poland, under research project No. UGB 822/2023.

REFERENCES

1. https://www.europarl.europa.eu/news/pl/headlines/society/20191129STO67756/emisje-z-samolotow-i-statkow-fakty-i-liczby-infografika; - no publication data (Accessed on 01.04.2023)
2. Merkisz J. Ekologia w lotnictwie, Instytut Silników Spalinowych i Transportu, Politechnika Poznańska, Poznań 2016. https://docplayer.pl/50676369-Ekologia-w-lotnictwie.html - (Accessed on 01.04.2023)
3. Jakubowski R. Spalanie-Emisja toksycznych zanieczyszczeń oraz metody jej ograniczania w nowoczesnych komorach spalania silników lotniczych; https://docplayer.pl/31360741-Spalanie-emisja-toksycznych-zanieczyszczen-oraz-metody-jej-ograniczania-w-nowoczesnych-komorach-spalania-silnikow-lotniczych.html - (Accessed on 01.04.2023)
4. European Aviation Environmental Report 2022, EASA 2022; https://www.easa.europa.eu/eco/

sites/default/files/2023-02/230217_EASA%20EAER%202022.pdf - (Accessed on 01.04.2023)

5. DSF-000008-A01-Initial-WAT WESTT-BR TRAINING; Price Induction's proprietary materials, 2017
6. Kozakiewicz A. Estymacja punktu pracy sprężarki i jego parametry w oparciu o charakterystyki sprężarek, WAT, Warszawa, 2016. DOI: 10.5604/05096669.1226207
7. Głowacki P., Szczeciński S. Turbinowy silnik odrzutowy jako źródło zagrożeń ekologicznych, Prace Instytutu Lotnictwa, Warszawa 2011; 4: 252–257.
8. Balicki W., Chachurski R., Głowacki P., Kawalec K, Kozakiewicz A., Pągowski Z., Szczeciński J., Szczeciński S. Lotnicze silniki turbinowe. Konstrukcja-Eksploatacja-Diagnostyka, Biblioteka Naukowa Instytutu Lotnictwa, Warszawa 2010; 428.
9. Balicki W., Chachurski R., Głowacki P., Kozakiewicz A., Szczeciński S., Ekologia na lotniskach. Przegląd Sił Zbrojnych, 2014; 3: 85–89.
10. Merkisz J., Markowski J., Pielecha J., Emission tests of the F100-PW-229 turbine jet engine during pre-flight verification of the F-16 aircraft, WIT Transactions on Ecology and The Environment. 2013; 174: 219–230. WIT Press, www.witpress.com, (on-line), https://www.witpress.com/Secure/elibrary/papers/AIR13/AIR13019FU1.pdf / Accessed on 2022-04-12/
11. Fulara S., Chmielewski M., Gieras M., Variable Geometry in Miniature Gas Turbine for Improved Performance and Reduced Environmental Impact, Energies. 2020; 13(5230): 1–19. DOI: 10.3390/en13195230
12. Kotlarz W. Turbinowe zespoły napędowe źródłem skażeń powietrza na lotniskach wojskowych, Wyższa Szkoła Oficerska Sił Powietrznych, Dęblin 2003; 177.
13. Kuźniar M., Orkisz M. Analysis of the Application of Distributed Propulsion to the AOS H2 Motor Glider. Journal of KONES Powertrain and Transport. 2019; 26(2): 85–92. DOI: 10.2478/kones-2019-0036
14. Kozakiewicz A., Grzegorczyk T. Electric aircraft propulsion, Journal of KONBiN. 2021; 51(4): 49–66. DOI: 10.2478/jok-2021-0044
15. Falkowski K., Kurnyta-Mazurek P., Szolc T., Henzel M. Radial Magnetic Bearings for Rotor–Shaft Support in Electric Jet Engine. Energies. 2022; 15: 3339. https://doi.org/10.3390/en15093339
16. Wheeler P., Sirimanna T.S., Bozhko S., Haran K.S. Electric/Hybrid-Electric Aircraft Propulsion Systems, proceedings of the IEEE. 2021; 109(6): 1115–1127. DOI: 10.1109/JPROC.2021.3073291
17. Kołodziejska A., Kozakiewicz A., Sibilski K. Jądrowy napęd statków powietrznych – idea, której czas nigdy nie powróci? Mechanika w lotnictwie, ML-XX 2022, https://doi.org/10.15632/ML2022/185-201
18. Bahr D.W. Technology for the Design of High Temperature Rise Combustors. J. Propulsion. 1987; 3(2): 179–186. https://doi.org/10.2514/3.22971
19. Makida M., Yamada H., Yamamoto T. Development of Full Annular Combustor for Small Aircraft Jet Engine in JAXA TechCLEAN Project, 26TH International Congress of The Aeronautical Sciences, ICAS. 2008; 1–10. https://www.icas.org/ICAS_ARCHIVE/ICAS2008/PAPERS/559.PDF, (Accessed on 2023-03-22)
20. Szczeciński S., Balicki W., Chachurski R., Głowacki P., Kozakiewicz A. Ekologia na lotniskach. Przegląd Sił Zbrojnych, 2014; 3: 85–89. https://zbrojni.blob.core.windows.net/pzdata/TinyMceFiles/PSZ_NR3.pdf, (Accessed on 2023-03-22)
21. Przysowa R., Gawron B., Białecki T., Ł¸egowik A., Merkisz J., Jasiński R. Performance and Emissions of a Microturbine and Turbofan Powered by Alternative Fuels, Aerospace 2021; 8: 25. https://doi.org/10.3390/aerospace8020025
22. Białecki T., Dzięgielewski W., Kowalski M., Kulczycki A. Reactivity Model as a Tool to Compare the Combustion Process in Aviation Turbine Engines Powered by Synthetic Fuels, Energies. 2021; 14: 6302. https://doi.org/10.3390/en14196302
23. Enis T. Turgut, Oznur Usanmaz, Marc A. Rosen, Empirical analysis of the effect of descent flight path angle on primary gaseous emissions of commercial aircraft. Environmental Pollution. 2018; 236: 226–235. https://doi.org/10.1016/j.envpol.2018.01.084
24. Zhang M., Filippone A. Optimum problems in environmental emissions of aircraft arrivals, Aerospace Science and Technology. 2022; 123: 107502. https://doi.org/10.1016/j.ast.2022.107502
25. Ekenechukwu C., Okafor K.D., Kunkuma A. Somarathne, Rattanasupapornsak Ratthanan, Akihiro Hayakawa, Taku Kudo, Osamu Kurata, Norihiko Iki, Taku Tsujimura, Hirohide Furutani, Hideaki Kobayashi, Control of NOx and other emissions in micro gas turbine combustors fuelled with mixtures of methane and ammonia. Combustion and Flame. 2020; 211: 406–416. https://doi.org/10.1016/j.combustflame.2019.10.012 0010-2180
26. Li M., Wang Q., Zhao Y., Dai X., Shang W. Combustion and emission characteristics of a novel staged combustor for aero gas turbine engine, Aerospace Science and Technology. 2023; 134: 108169. https://doi.org/10.1016/j.ast.2023.108169
27. Mahto N., Satyanarayanan R. Chakravarthy S.R. Response surface methodology for design of gas turbine combustor. Applied Thermal Engineering. 2022; 211: 118449. https://doi.org/10.1016/j.applthermaleng.2022.118449